Spatiotemporal dynamics of actin-rich adhesion microdomains: influence of substrate flexibility

Olivier Collin[1], Philippe Tracqui[1,*], Angélique Stephanou[1], Yves Usson[2], Jocelyne Clément-Lacroix[1] and Emmanuelle Planus[1,*,‡]

[1]Equipe DynaCell and [2]Equipe RFMQ, Laboratoire TIMC-IMAG, CNRS UMR5525, Institut de l'Ingénierie et de l'Information de Santé-Faculté de Médecine, 38706 La Tronche CEDEX, France

*Authors for correspondence (e-mail: emmanuelle.planus@ujf-grenoble.fr; philippe.tracqui@imag.fr)
‡Present address: Laboratoire LEDAC, UMR CNRS-UJF 5538, Institut Albert Bonniot 38706 La Tronche CEDEX, France

Accepted 15 December 2005
Journal of Cell Science 119, 1914-1925 Published by The Company of Biologists 2006
doi:10.1242/jcs.02838

Summary

In this study we analyse the formation and dynamics of specific actin-rich structures called podosomes. Podosomes are very dynamic punctual adhesion sites tightly linked to the actin cytoskeleton. Mechanical properties of substrates are emerging as important physical modulators of anchorage-dependent processes involved in the cellular response. We investigate the influence of substrate flexibility on the dynamic properties of podosomes. We used mouse NIH-3T3 fibroblasts, transfected with GFP-actin and cultured on polyacrylamide collagen-coated substrates of varying stiffness. Static and dynamic features of cell morphologies associated with an optical flow analysis of the dynamics of podosomes revealed that: (1) they have constant structural properties, i.e. their shape factor and width do not change with the substrate flexibility; (2) the lifespan of podosomes and mean minimum distance between them depend on the substrate flexibility; (3) there is a variation in the displacement speed of the rosette of podosomes. Moreover, the rosettes sometimes appear as periodically emergent F-actin structures, which suggests that a two-level self-organisation process may drive first, the formation of clusters of podosomes and second, the organisation of these clusters into oscillating rings. Such dynamic features give new perspectives regarding the potential function of podosomes as mechanosensory structures.

Supplementary material available online at
http://jcs.biologists.org/cgi/content/full/119/9/1914/DC1

Key words: Podosomes, Matrix stiffness, Self-organisation, Optical flow

Introduction

Actin dynamics are largely involved in cell migration, which is a major process in the biology and physiopathology of morphogenesis, wound healing and carcinogenesis. Cell locomotion consists of repeated cycles of adhesion and de-adhesion to the substrate (Lauffenburger and Horwitz, 1996). Moving cells can exhibit different types of adhesion (Kaverina et al., 2002) such as focal adhesions (Petit and Thiery, 2000), fibrillar adhesions (Zamir et al., 1999), focal complexes (Nobes and Hall, 1995) or podosomes (Linder and Aepfelbacher, 2003), where actin is a common component of the protein scaffold. All these scaffolds are involved in signalling interactions with the extracellular matrix (ECM) on the outside and with the actin cytoskeleton in the cell interior, through transmembrane receptors of the integrin family (Schoenwaelder and Burridge, 1999). They are also associated with specific assembly of actin filaments and their formation and maintenance depend on the stress level within the actin cytoskeleton. This paper focuses on one of the specialised adhesion foci quoted above – the podosome. Like focal adhesions, podosomes include several proteins: integrin, paxillin, vinculin and talin but their structural organisation and dynamical appearance are different. Initially described by David-Pfeuty and Singer in fibroblasts transformed by rous sarcoma virus (David-Pfeuty and Singer, 1980), podosomes are single adherent points. They are formed by a dense actin core, organised as a column of small actin filaments, and surrounded by adhesion proteins (integrins) and scaffolding proteins, such as cortactin (Destaing et al., 2003), PyK2 (Pfaff and Jurdic, 2001), WASP (Calle et al., 2004) and gelsolin (Chellaiah et al., 2000). Podosomes do not move, but they are very dynamic structures, dissolving and then reforming in new locations with a life span ranging from 2 to 12 minutes (Kanehisa et al., 1990). The appearance and disappearance of a great number of podosomes within a cell can generate specific patterns such as clusters, bands, belts or rosettes (reviewed by Linder and Apfelbacher, 2003). In recent times, podosomes have been observed in an increasing number of cell types, but little is known about their roles. They appear to be dynamic structures important for cell adhesion and substrate degradation. They are indeed typically found in invasive cells and in cells that cross tissue boundaries (Burgstaller and Gimona, 2005; Chen, 1989). Podosomes are also constitutively found in osteoclasts where their role begins to be elucidated. In mature osteoclasts, the rosettes of podosomes are organised in a peripheral belt which hypothetically could mature into a sealing zone (Destaing et al., 2003). More recently, it has been shown that podosomes do not mature into a sealing zone, as both structures are formed independently and on different substrates (Saltel et al., 2004). This sealing zone is defined as a unique large band of actin

which allows cell attachment on the mineralised bone matrix and thus creates a sealed area where enzymes and protons are confined, leading to an increasing bone resorption. In summary, rosettes are adherent dynamic structures associated with polymerisation and depolymerisation of actin filaments. Consequently the podosomes provide an attractive in vitro model to study how the extracellular matrix flexibility controls actin dynamics through the adhesion sites in living adherent cells.

Indeed, it has been shown that the extracellular matrix rigidity plays a crucial role in several cellular processes, ranging from locomotion (Lo et al., 2000; Pelham and Wang, 1997), to anchorage dependency of growth control (Burridge and Chrzanowska-Wodnicka, 1996; Chen et al., 1997; Folkman and Moscona, 1978), phagocytosis (Beningo and Wang, 2002), differentiation (Cukierman et al., 2001; Deroanne et al., 2001) and ECM remodelling (Mudera et al., 2000; Tranqui and Tracqui, 2000; Urech et al., 2005). Since the rosettes of podosomes are adherent structures, we investigate the influence of the matrix rigidity on the dynamic properties of these structures in 3T3 fibroblasts transfected with GFP-actin. In this study, we used bio-functional polyacrylamide substrates (Pelham and Wang, 1998), whose stiffness is controlled by altering the ratio between monomer and cross-linker concentrations. Two different ratios of bis-acrylamide:acrylamide were used to define flexible and very flexible substrates, with glass defined as a reference rigid substrate. Stably transfected 3T3 fibroblasts allowed us to track by videomicroscopy the spatiotemporal dynamics of the specific adherent actin structures called rosettes, assembled from numerous individual podosomes. Image analysis shows that both the podosome lifespan and the minimum distance between podosomes depend on the substrate flexibility, leading to a variability of the rosette dynamics. Moreover, an optical flow analysis demonstrates the occurrence of a periodic appearance and disappearance of the rosettes, allowing us to postulate the self-organised nature of these actin-rich adhesion micro-domains. Thus, rosettes could have a role as a fast-moving mechanosensor organelle.

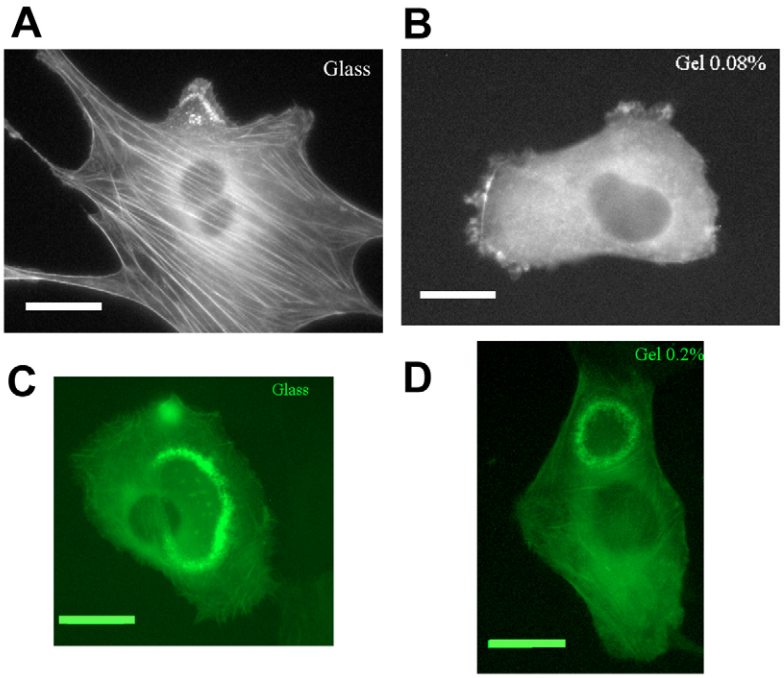

Fig. 1. Actin cytoskeleton structure and podosome rosette appearance of spread 3T3 fibroblasts depend on substrate flexibility. 3T3 GFP-actin transfected fibroblasts observed by fluorescence microscopy. A 3T3 fibroblast spread on rigid substrate (glass) exhibits a larger number of actin stress fibres (A) than a fibroblast on very flexible substrate (0.08% bis-acrylamide) (B). The cell appears more spherical and loses most of its actin stress fibres on 0.08% gel. However 3T3 fibroblasts can exhibit podosome rosettes, i.e. large ring-shaped bands made of an actin cloud surrounding dense actin dots on both rigid (C) and flexible substrates (D) (0.2% gel), although the frequency of appearance of the rosettes is higher for rigid substrates than for flexible ones. Bars, 10 μm.

Results

Cell cytoskeleton (CSK) morphology on very flexible, flexible and rigid substrates

We first compared the actin CSK morphology of 3T3 fibroblasts adherent on environments with varying flexibility. On rigid and flexible substrates, i.e. glass and 0.2% bis-acrylamide gel, 3T3 fibroblasts are well spread and exhibit a large number of actin stress fibres (Fig. 1A). When the cells are cultured on very flexible substrates, 3T3 cells adopt more spherical morphologies and lose most of their stress fibres (Fig. 1B). These data are consistent with previous studies (Pelham and Wang, 1997; Yeung et al., 2005). However, whatever the substrate flexibility, 3T3 fibroblasts exhibit highly dynamic rings of dense actin dots (Fig. 1C,D). These actin rings, named rosettes, appear more frequently when cells are spread on rigid substrates. It was consequently more difficult to observe these structures on very flexible substrates. Remarkably, these transient actin-based structures, organised in rosettes, exhibit different dynamic properties according to the substrate flexibility. All these observations indicate a close relationship between actin dynamics and mechanical properties of the substrate in cell adhesion. The dynamics of these actin structures were thus analysed at different levels: (1) structure and dynamics of the podosomes forming these particular actin constructions; (2) structure and dynamics of the clusters of podosomes in cells adhering to very flexible, flexible and rigid substrates.

Structure and dynamics of podosomes: dependence on the substrate flexibility

Close observation of the transient actin-based structures organised in rosettes or clouds in GFP-actin 3T3 fibroblasts reveals that these structures are formed by podosomes (actin dots) (Fig. 2A). Observations with fluorescence video microscopy and with confocal interference reflection microscopy (CIRM), showed that these localised actin structures correspond to adhesion sites onto the substrate (Fig. 2B). Indeed, the points observed by fluorescence match exactly the zones of close contact between the basal cell membrane and the substrate (David-Pfeuty and Singer, 1980). Individual podosomes can organise collectively to form a rosette (Fig.

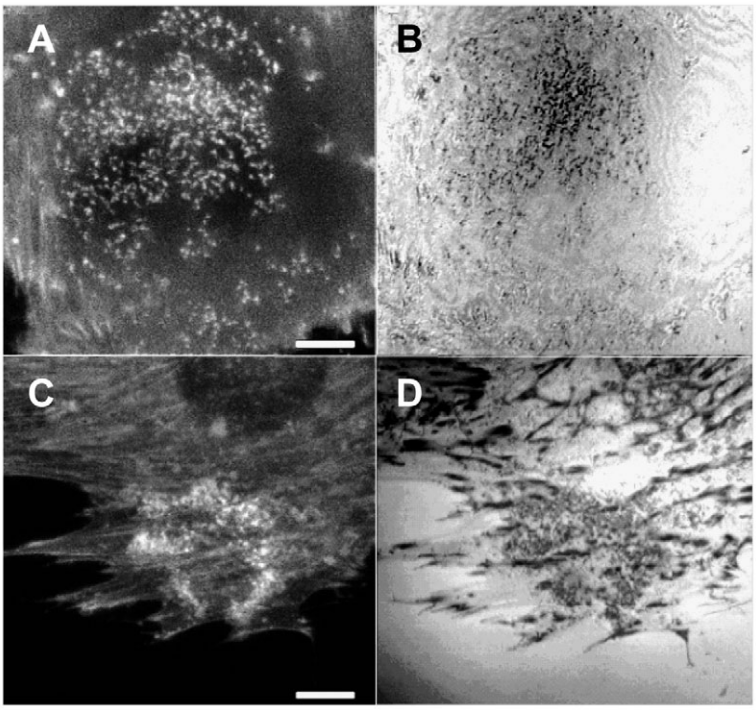

Fig. 2. Podosome rosettes are adherent structures. (A) Observation of 3T3 fibroblasts by total internal fluorescence microscopy show that podosomes are dense actin dots. (B) Confocal interference reflection microscopy (CIRM) revealed that podosomes are structures in close contact with the substrate and are therefore involved in cell adhesion. (C) Rosette in 3T3 fibroblast viewed by fluorescence. This ring-shaped structure is composed of a large number of podosomes, all adherent to the substrate (D), as observed with CIRM. Furthermore, they can coexist with other adherent structures such as focal contacts. Bars, 10 μm.

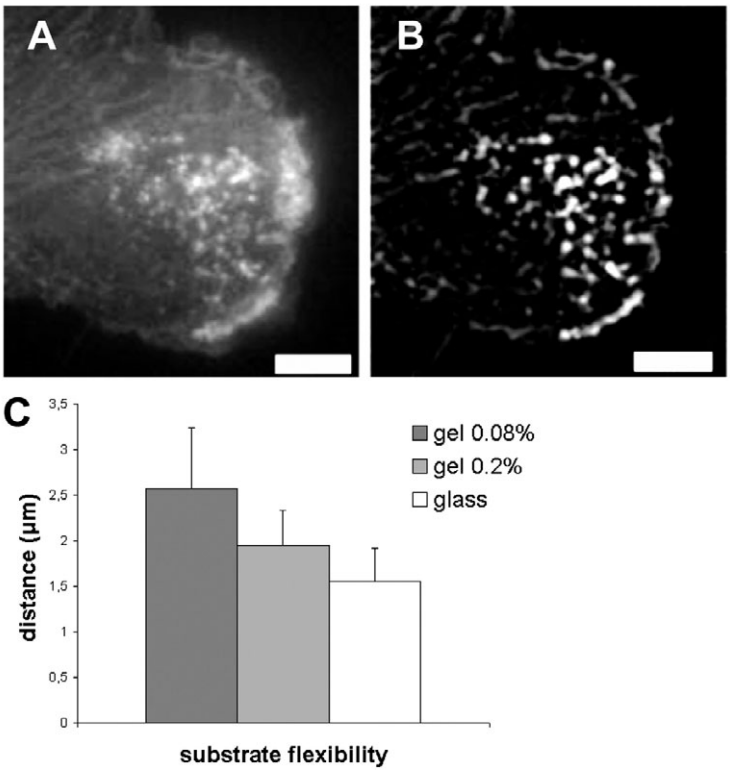

2C,D). Moreover, they can coexist with other adhering structures, especially with focal adhesions that cells develop to adhere more firmly to the substrate.

Fluorescence microscopy shows that podosomes organised in rosettes are surrounded by an actin cloud. In order to focus on the podosome properties, we used image a top-hat filter (Schamber, 1978) to post-process the image sequences (Fig. 3A,B). We first emphasised the podosome organisation in rosettes in relation to the substrate flexibility and measured the mean distance between neighbouring podosomes. This was done for 16 distances per rosette appearing in a cell over the time of existence of this rosette, and averaged for about 10 cells for each type of substrate flexibility. Results show a decrease of the mean distance between neighbours with increasing substrate rigidity (Fig. 3C). These mean distance value is 2.57±0.66 μm for 0.08% gel, falling to 1.95±0.38 μm for 0.2% gel and to 1.53±0.36 μm for the reference rigidity, i.e. glass. Assuming the statistical distribution of these distances follows a normal law for each class of gel, we ran a Student's *t*-test, and show that differences between mean distances are significant ($P \ll 0.0001$).

Podosome cluster and rosette motions result from the interplay of podosome assembly and disassembly. By tracking one given podosome just after its appearance, we calculated its lifespan until it disappeared (Fig. 4A-E). Lifespan estimation was made on 12 podosomes for each rosette in a cell and evenly averaged for ~10 cells for each type of substrate. Results show that podosomes are more stable on a more rigid substrate: their lifespan increased from 1 minute 24±38 seconds (0.08% gel) to 2 minutes 40±73 seconds (glass) with an intermediate lifespan of 1 minute 53±47 seconds for 0.2% gel (Fig. 4F). Student's *t*-tests revealed that these mean differences are significant ($P \ll 0.0001$).

Structure of podosome clusters: the rosette level

Podosomes are mostly clustered in ordered groups, which undergo constant rearrangements. In our GFP-actin 3T3 cell model, numerous individual podosomes formed a rosette than can contract, relax, move or disappear. This phenomenon emerges whatever the rigidity of the substrate we used. However, the probability of appearance is not the same: one can easily observe rosettes on rigid substrates, but they occur less frequently on flexible

Fig. 3. The distance between neighbouring podosomes depends on the substrate flexibility. (A) Total internal fluorescence microscopy of a podosome cluster. Podosomes are hardly visible over the dense actin cloud. (B) Image post-processing by a top-hat filter reveals the location of podosomes. Bars, 10 μm. (C) Computation of the mean distance between nearest podosomes for 16 pairs of podosomes per cell over full time-lapse sequences and for each substrate rigidity (n=96 for 0.08% gel; n=112 for 0.2% gel; and n=144 for glass). Data are expressed as mean ± s.d.

substrates. The rosette organisation can appear everywhere in the cell, at the cell periphery as well as in more central locations. Nevertheless, they rarely appear below the nucleus. Observations along the *Z* axis with confocal microscopy show that the rosettes are thick structures with a depth ranging from 2 to 3 μm (data not shown), which explains the scarcity of the phenomenon under the nucleus on well-spread cells.

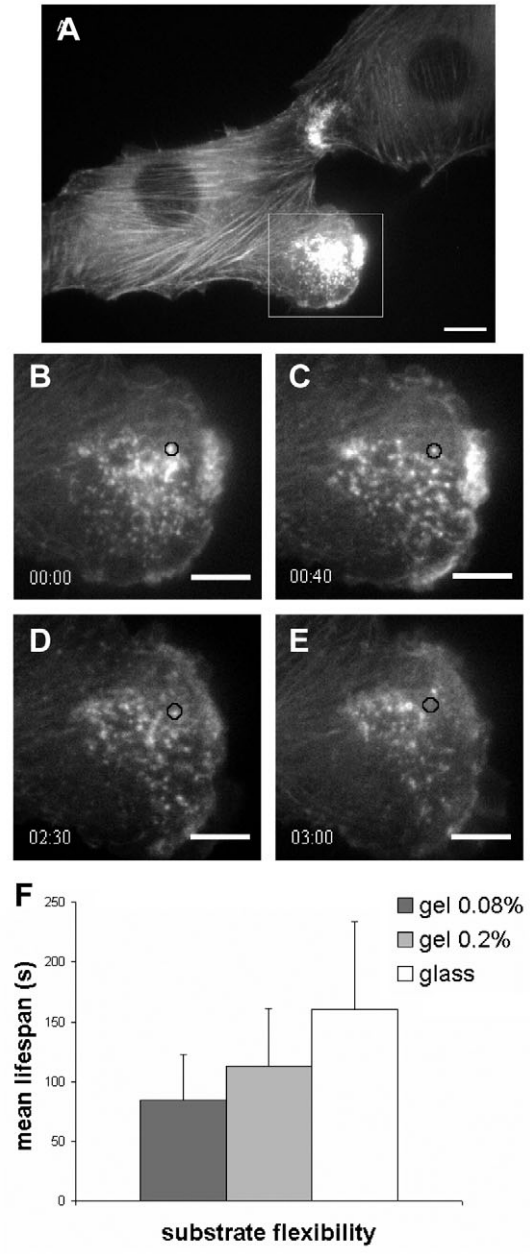

Fig. 4. Individual podosome lifespan depends on the substrate flexibility. (A) 3T3 fibroblast observed by fluorescence microscopy exhibiting an actin cluster. (B-E) Movement of the cluster over 3 minutes revealed an apparent motion induced by appearance and disappearance of non-moving podosomes (circled). (F) The lifespan of podosomes calculated by averaging the lifespan of about ten podosomes per cell, and for each substrate type (n=68 for 0.08% gel; n=63 for 0.2% gel; and n=99 for glass). Data are expressed as mean ± s.d. Bars, 20 μm (A); 10 μm (B-E).

Rosettes can be closed or more rarely appear as open bands. The rosette shape factor, defined as the ratio of the large axis over the small axis of the rosette, ranges from 1 to 2. Rosettes are also highly symmetrical structures whatever the cell shape. We calculated the width of the band for each rosette as the average of four points, and this was done for five cells for each type of substrate flexibility. Unexpectedly, the width (w) was highly constant (w≈4 μm) for all the rosettes and did not vary significantly with substrate flexibility: 3.93±0.41 μm for glass, 4.02±0.93 μm for flexible gel and 4.36±1.21 μm for very flexible gel (P>0.05). Also, it is important to observe that it can be easy to distinguish individual podosomes from the surrounding cloud of mostly monomeric actin molecules when podosomes rosettes were adherent to rigid substrate (i.e. glass), this become more difficult when the substrate flexibility increased (see Fig. 5A,B). To determine whether this observation is an intrinsic property of podosome rosettes adherent to a flexible substrate or is an optical effect owing to diffusion of emission fluorescence when passing through the polyacrylamide gel, we have quantified the FITC fluorescence from beads with the same diameter as the podosomes (i.e. 0.5 μm) and spread these over the gel. The beads were then covered with a glass coverslip and the fluorescent observations were made either

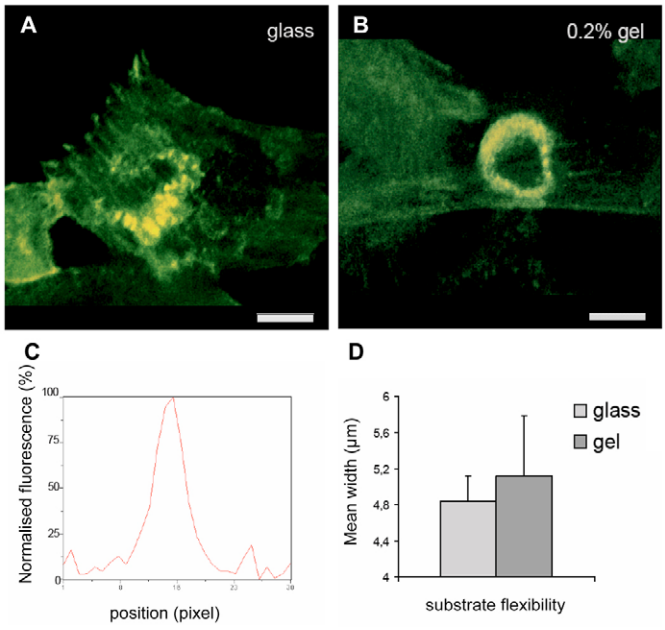

Fig. 5. Podosomes are more stable and more individualised on rigid substrates. Podosome rosette observed by confocal microscopy for actin GFP in a 3T3 cell seeded on rigid (A) and flexible substrate (B). The 3D reconstruction was made by measuring fluorescence density. High-density regions were coloured in red whereas weaker densities were coloured in green. The rosette on the rigid substrate is composed of individual actin dots covered by a weak actin cloud. (B) When seeded on flexible substrate, the rosette appears more blurred and actin dots are very difficult to distinguish from the denser actin cloud. Bars, 10 μm. (C) Line scan of the fluorescence profile of FITC beads when spread on polyacrylamide gels, allowing the computation of the width at half height of the main peak. (D) Mean width for glass and flexible substrates illustrates the optical diffusion caused by the gel (n=20).

through the gel or through the coverslip. The light diffusion was quantified by measuring the mean width at half-height of the main fluorescence peak (Fig. 5C). The mean width when measured through the glass coverslip is 4.82±0.28 μm and slightly increased to 5.11±0.67 μm when measured through the gel (Fig. 5D). Light diffusion is also a minor effect, meaning that the complexity of individualisation of the podosomes is not an optical effect and the actin cloud is denser when substrate flexibility increases.

Dynamical properties of the rosette: dependence on the substrate flexibility

Rosettes seem to emerge from an actin core that grows and evolves into a ring-shaped structure with constant width as soon as it reaches a certain size. It can then move inside the cell or remain very stable spatially, growing in size and then shrinking, sometimes periodically, or disrupting and giving birth to a rotating wave. This variety of dynamic patterns can appear on every substrate, whatever their flexibility. An accurate observation showed that the rosette moves globally whereas podosomes remain fixed on the substrate. This motion thus appears to be an apparent movement linked to the assembly and disassembly of podosomes. In order to investigate the dynamics of actin podosome rosettes, we carried out FRAP experiments. This method enabled us to quantify the variation of fluorescence in a narrow section of the rosette. The corresponding fluorescence recovery rate was calculated in a close area surrounding the rosette, even if laser bleaching occurred all along the observed region (Fig. 6A,B). The fluorescence recovery in the rosette fitted closely an exponential law with a characteristic time constant τ ranging from 5 seconds to 20 seconds (Fig. 6C). This indicates that the rosette is at the centre of a very rapid actin turnover phenomenon.

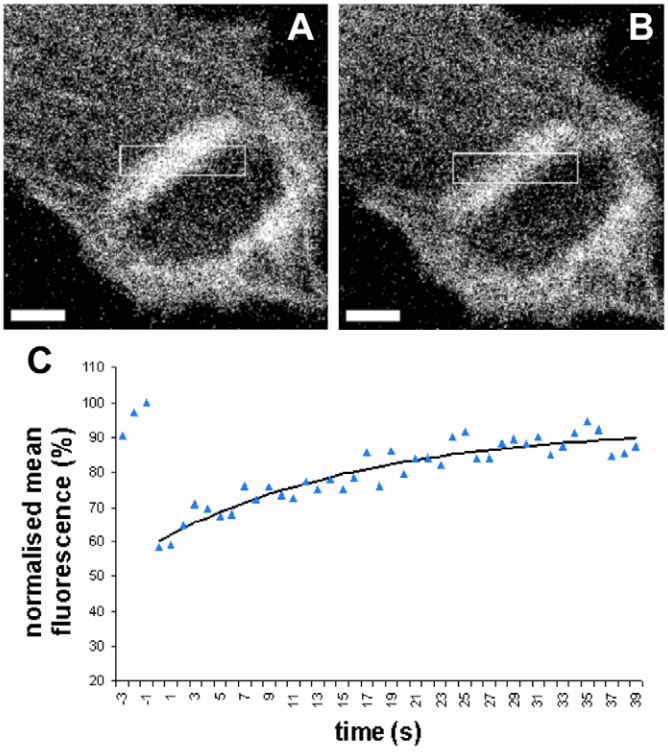

Fig. 6. FRAP analysis of the rosette. (A) The rosette before photo bleaching. A region of interest (ROI) is boxed in the rosette band. (B) After photobleaching the recovery of fluorescence in the ROI was measured. Bars, 10 μm. (C) Experimental data with an exponential recovery. The identified characteristic time is 17 seconds.

Quantification of rosette deformation

Optical flow analysis was performed on a population of 24 rosettes observed from 22 cells cultured on the three types of substrate. Several rosettes were observed simultaneously in the same cell only with a rigid substratum. Quantification of the rosette deformation is realised from the computation of the four coefficients E, ω, S_1 and S_2 that describe the expansion/contraction, the rotation, the horizontal and oblique shear rates respectively. Fig. 7 is a typical example of the observed rosette dynamics, showing the simultaneous evolution of the coefficients E, ω and S_1 and S_2 (Fig. 7A,B). The rosette exhibits a short expansion ($E>0$) immediately followed by a contraction phase ($E<0$), ultimately ending with the rosette extinction ($E=0$). The rotation component characterised by ω is mainly positive, resulting in a counter-clockwise rotation of the rosette. However, this component remains small during the expansion/contraction phases, compared with the other components, especially the shear rates. Fig. 7C,D shows the displacement fields corresponding to the two extremes of the expansion/contraction curve $E(t)$, namely the maximum expansion rate, which correlates in that case with a horizontal shear contraction ($S_1<0$) and the maximum contraction rate, which correlates with a horizontal shear expansion ($S_1>0$). Despite high horizontal shear rates, the rosette shape is globally conserved as $S_1(t)$ presents a 'balanced' profile where the horizontal expansion and contraction phases compensate each other.

Similar variations with time of the deformation coefficients were observed in: (1) six cases where a single expansion/contraction phase is followed by the rosette disappearance; (2) seven cases where rosette contraction is followed by its disappearance; and (3) one case where the rosette expands. We are especially interested here in the expansion/contraction parameter $E(t)$, which quantifies the speed of expansion or shrinking of the rosettes. We analysed the mean value of $E(t)$ during expansion and contraction over the different cases and for each substrate flexibility. Calculations were made on eight expansion/contraction phases on 0.08% gel, ten phases on 0.2% gel and 16 phases on glass. Results show that this rate varies with flexibility, decreasing from 0.081±0.05 second^{-1} for 0.08% gel to 0.038±0.02 second^{-1} for 0.2% gel and 0.014±0.003 second^{-1} for glass (Fig. 7E). Accordingly there is a decrease of the rosette mean velocity from 1.12 μm/minute for 0.08% gel to 0.52 μm/minute for 0.2% gel and 0.3 μm/minute for glass. The Student's t-test showed that these differences are significant ($P<0.03$).

Interestingly, the coexistence in the same cell and at the same time of two polymerised actin structures at the substrate-cell interface, namely actin stress fibres and podosome rosettes, have been observed. It is known that the time scales of the two actin structures are completely different, stress fibres associated with focal contacts being very stable, with lifespans in the order of hours, whereas podosomes in these cells, have

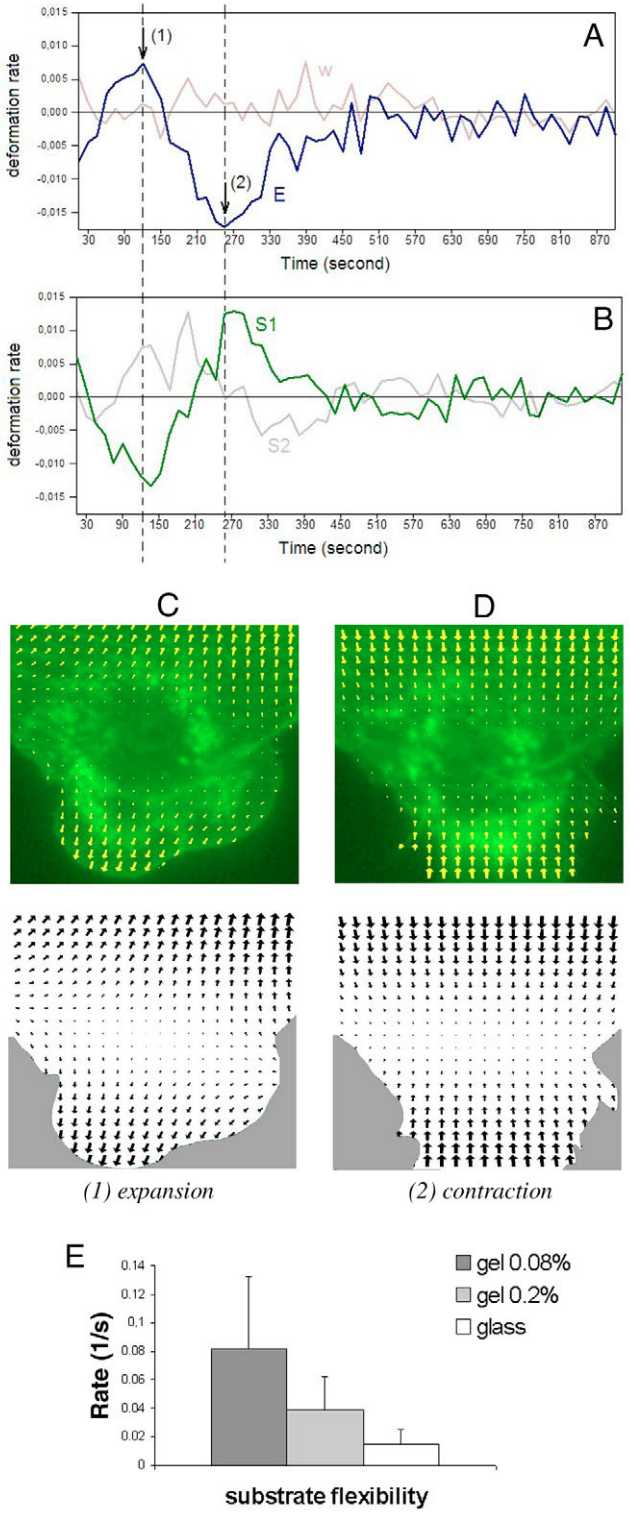

Fig. 7. Spatial dynamics of the rosettes depends on substrate rigidity. Simultaneous evolution with time of the expansion/contraction rate E (blue curve) and of the rotation rate ω (grey curve). (B) Simultaneous evolution of the orthogonal shear rate S_1 (green curve) and of the oblique shear rate S_2 (grey curve). (C) Velocity field superimposed to the rosette image at time t=120 seconds, which corresponds to the maximum expansion rate (1); (D) Velocity field superimposed to the rosette image at time t=255 seconds which corresponds to the maximum contraction rate (2). This rosette was observed on a rigid substratum (glass). (E) Mean rate of expansion and contraction averaged over several rosettes and for each value of substrate rigidity computed by n=8 for 0.08% gel; n=7 for 0.2% gel; and n=16 for glass. Data are expressed as mean ± s.d.

a very short lifespan: in the order of minutes. Fig. 8 shows that podosome rosettes can survive for minutes and move in the cell with no visible interaction with stress fibres. When the rosette approaches the membrane edges, this ring carries on evolving and the actin wave pushes the membrane. The ring then shrinks and leaves behind radial actin fibres that can drive the membrane retraction to its initial position.

Temporal analysis of rosette dynamics: emergence of periodic behaviour

A sample of ten rosettes exhibiting oscillating deformations was analysed by computing for each rosette the Fourier transform of the related expansion/contraction curve $E(t)$ to detect any potential periodicity in the signals. The sample of rosettes we studied was composed of seven rosettes observed with cells cultured on rigid substrate and three rosettes observed with cells cultured on flexible substrate (no oscillating deformation profiles were observed on cells cultured on very flexible substrates).

The search for a periodic component in the signals was realised regardless of the pattern of the rosette deformation. Indeed, Fig. 9 presents three different types of periodic deformation profiles. Fig. 9A shows a contraction profile without any rosette expansion, meaning that the rosette gradually shrinks. Fig. 9C shows a periodic oscillation with alternating phase of expansion and contraction whose amplitude gradually decreases, meaning that the rosette gradually shrinks through damped oscillations. Fig. 9E shows a similar oscillation profile with decreasing amplitude, but characterised by asymmetrical expansion and contraction phases: the expansion phase is slow (about 300 seconds) whereas the shrinking phase is more than three times faster (around 75 seconds), until the signal amplitude decreases once again. Although these signals are different in nature, the temporal Fourier transform analysis performed in each case (Fig. 9B,D,F), shows the appearance of maxima in the signals amplitude for almost exactly the same frequency: the double peak in Fig. 9B at 0.0029 and 0.0051 Hz gives an estimated period of 4 minutes 28 seconds (±1 minute 42 seconds) and the two single peaks in Fig. 9D,F both at 0.036 Hz, correspond to an estimated period of 4 minutes 36 seconds (±10 seconds). The results obtained for the ten oscillating profiles gave two signals with no periodicity, three signals with a mean period of 2 minutes 14±26 seconds and five signals with a mean period of 4 minutes 27±37 seconds. It is important to note that this latter value is twice the mean period of 2 minutes 14 seconds. This suggests that the largest period could result from an amplification of a process occurring at a smaller timescale.

All together, the results we obtained seem to show that the substrate flexibility has no influence on the periodicity of rosette deformation dynamics: signals with no periodicity can appear on the three different types of substrates. On the two substrates where we observed periodic signals, periods of 2 minutes and periods of 4 minutes appeared on both substrates.

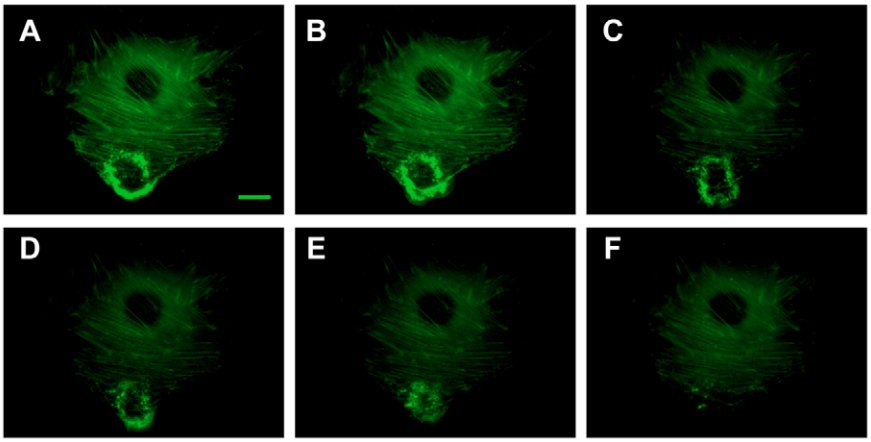

Fig. 8. Motion of the rosettes is associated with the protrusion of the cell membrane. (A-F) 3T3 cell exhibiting growth and shrinkage of a rosette over 5 minutes with time intervals of 1 minute. The movement of the rosette along the cell periphery allows protrusion and retraction of the membrane as it grows and shrinks. Bar, 10 μm.

Therefore no discrimination of the oscillating rosette behaviour can be made with respect to the substrate flexibility.

Role of the cytoskeleton in rosette formation and dynamic

In order to probe the role of the cytoskeleton in the morphogenesis of podosome rosettes, we applied various agents that disrupt actin and microtubules polymers, and a specific agent to inhibit myosin. The drugs were applied when cells were initially exhibiting podosome rosettes. We induced actin depolymerisation by using cytochalasin D (cytoD) (Fig. 10A,B). Under cytoD treatment and during the extension of the rosette of podosomes we observed that the actin wave expansion is rapidly stopped. Moreover, the podosomes

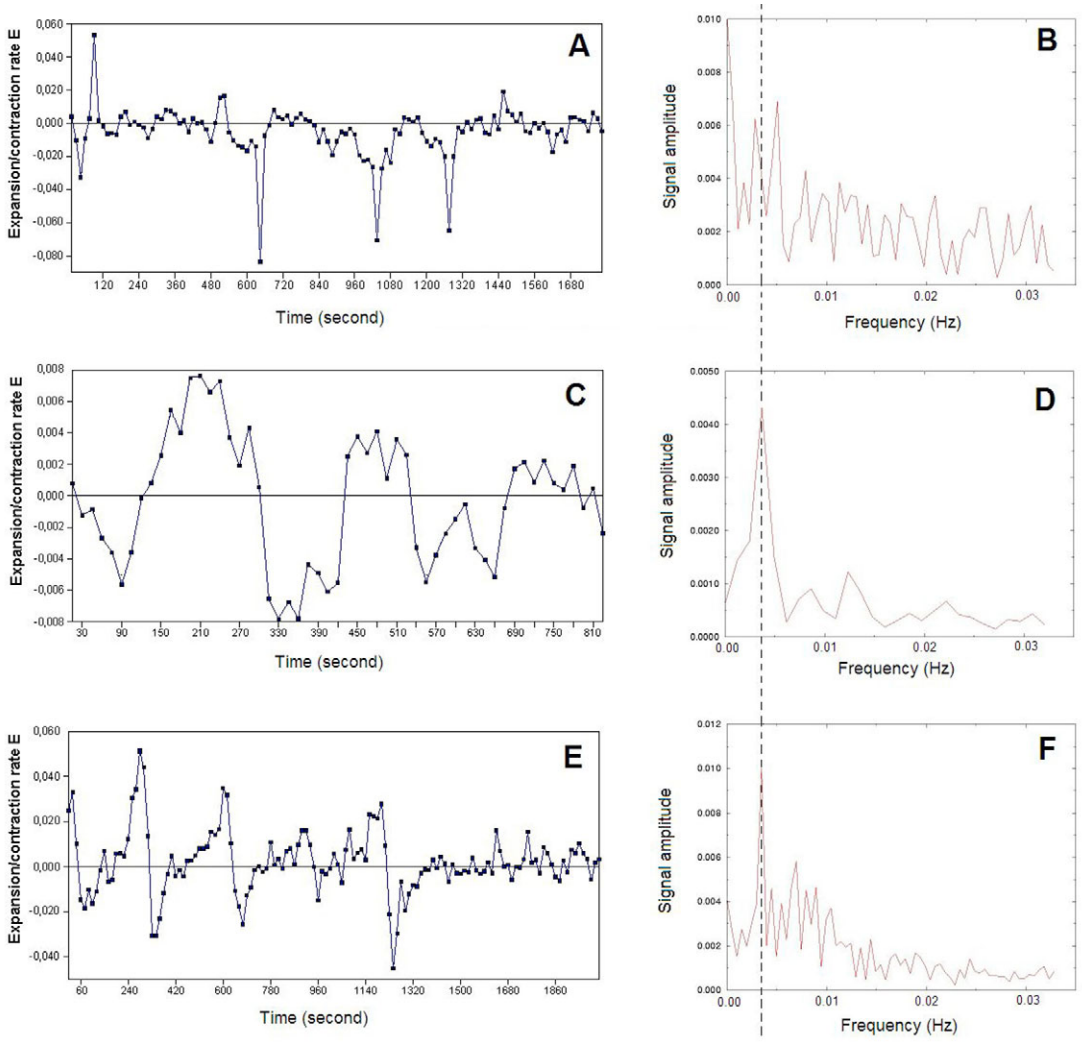

Fig. 9. Podosome rosettes can be a periodically emerging structure. (A,C,E) Diversity of the profiles exhibited by expansion/contraction rates $E(t)$. (A) Contraction profile without rosette expansion (on flexible substratum). (C) alternating symmetrical expansion and contraction phases with decreasing signal amplitude (on rigid substratum). (E) Alternating asymmetrical expansion and contraction phases with decreasing signal amplitude (on rigid substratum). (B,D,F) Associated Fourier transforms of the $E(t)$ time series in A-C, respectively.

forming the rosette remained in their position for several minutes (Fig. 10C,D). After 30 minutes of incubation with cytoD, rosettes and podosomes are no longer visible. It is known that microtubules stabilise podosome patterns (Babb et al., 1997, Linder et al., 2000) and the role of microtubules in rosette formation and their persistence was investigated using nocodazole (Fig. 10E and F). We treated the 3T3 GFP-actin fibroblasts for increasing incubation times with nocodazole and this treatment had no effect on rosette formation nor on their persistence in our cellular model. This result suggested that there is no influence of microtubules on the enlarged distance between podosomes on flexible substrate. This is not surprising because it has already been shown on mouse macrophages that de novo assembly of podosomes is not dependent on microtubules whereas the fusion and fission rates of larger precursor structures are based on microtubule dynamics (Evans et al., 2003). Also, as previously demonstrated for osteoclasts (Destaing et al., 2003) depolymerising microtubules had no effect on the existence of rosettes in 3T3 fibroblasts. Actually, these authors have demonstrate that a functional microtubule network was needed to stabilise the podosome belts at the cell periphery in osteoclasts, but at early stages of osteoclast differentiation, microtubule depolymerisation by nocodazole treatment had no visible effect on podosome clusters and rosettes.

Finally, to investigate the role of actomyosin contractility in podosome formation and persistence, we used two myosin inhibitors, 2,3-butanedione monoxime (BDM), an inhibitor of the myosin motor (Pelham and Wang, 1997), and blebbistatin (Bb), a specific inhibitor of class II myosins (Shu et al., 2005). After application, BDM rapidly induced the disappearance of the podosomes (Fig. 10G,H) and a strong reshaping of the cell body occurred, resulting in a rounded cell within 20 minutes. BDM is a well-characterised, low-affinity, non-competitive inhibitor of skeletal muscle myosin II, but has a broad effect on many non-myosin proteins (many uncharacterised) (Ostap, 2002), and we next tested a more specific myosin inhibitor. Blebbistatin was used at increasing concentrations from 50 μM to 100 μM. Applying 75 μM or more caused a dramatic effect on 3T3 GFP-actin fibroblasts leading to a massive cell lysis after only 20 minutes. We observed a less drastic effect for a Bb concentration of 50 μM, where podosomes disappeared after 10 minutes, whereas the cells kept their stress fibres for at least 30 minutes (Fig. 10I,J). Since Bb is a reversible inhibitor, we observed the reorganisation of podosome rosettes 24 hours after an intense washing of the preparation (data not shown).

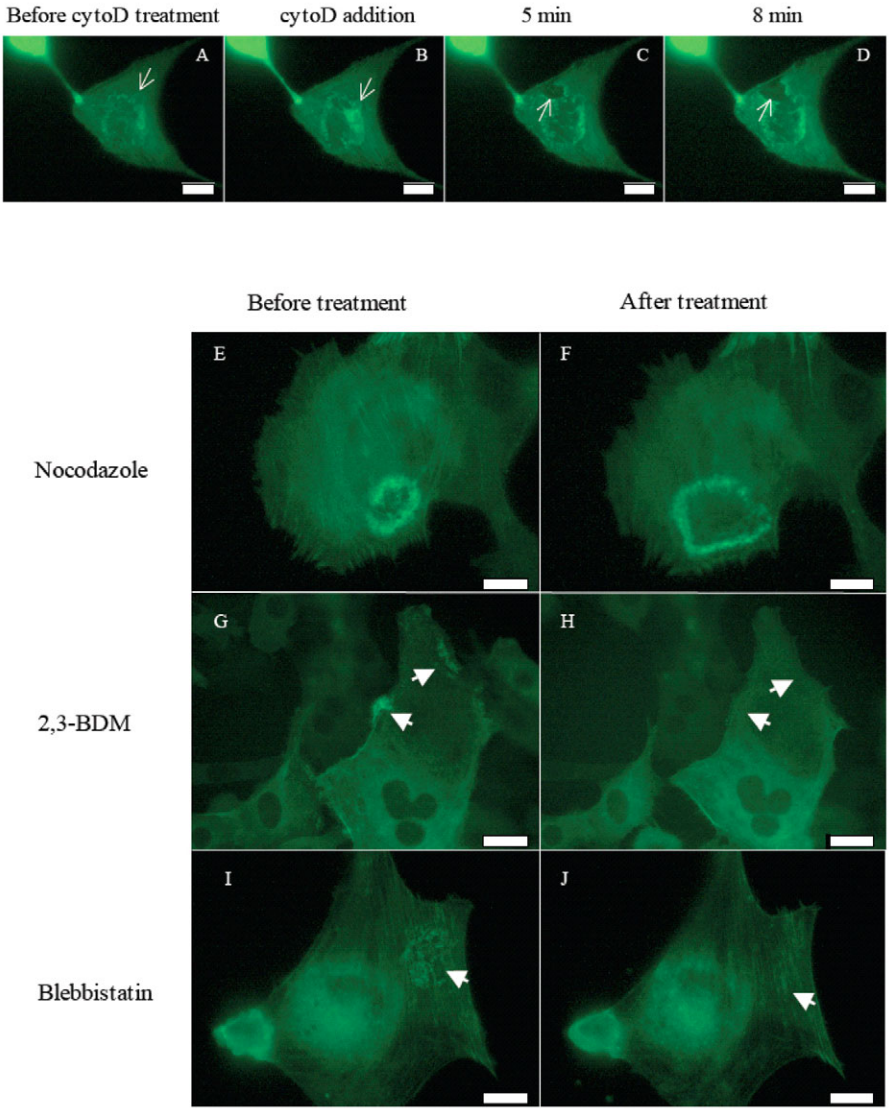

Fig. 10. Effect of drug treatment on podosome dynamics. 3T3 fibroblasts spread on glass exhibit a podosome rosette visualised by GFP actin fluorescence. (A-D) Soon after treatment, cyto D inhibits actin wave propagation (B, arrow). Five minutes after treatment, the actin cytoskeleton disrupts, inhibiting new podosome formation. Podosomes previously formed stay still for several minutes in their position during actin disruption (C,D, arrows). Depolymerising the microtubule cytoskeleton using nocodazole has no effect on rosette propagation (E,F). Myosin inhibition with 2,3-BDM (G,H) or blebbistatin (I,J) completely inhibits podosome rosettes (arrows). Bars, 10 μm.

Discussion

Podosomes are found in many cells types in vitro, ranging from macrophages and osteoclasts (Destaing et al., 2003), to less-motile cells such as endothelial cells (Moreau et al., 2003), epithelial cells (Spinardi et al., 2004) vascular smooth muscle cells (Kaverina et al., 2003) and fibroblasts (Tarone et al., 1985). Individually, podosomes can be depicted as an actin core surrounded by actin-associated proteins such as α-actinin, vinculin, paxillin and talin embedded in a ring structure of integrins, and specific

proteins of the podosomes such as cortactin (Pfaff and Jurdic, 2001; Linder and Aepfelbacher, 2003; Linder and Kopp, 2005). In Src-transformed fibroblasts (Tarone et al., 1985), RSV-transformed BHK cells (Gavazzi et al., 1989), endothelial cells (HUVEC) (Osiak et al., 2005) and in the NIH 3T3 GFP-actin fibroblasts we used, podosomes organise together and form specific ring-shaped structures called rosettes which move in the cell at the substrate attachment side. In this study we characterised the dynamic properties of the rosette of podosomes and the relationships between these properties and the substrate rigidity. Note that we are dealing with an apparent motion of the rosettes because of the spatial stability of the podosomes themselves: they are temporarily adherent structures, assembling and disassembling with a specific lifespan in the order of one minute. It is their appearance and disappearance, which gives the feeling of a motion of the rosette.

In 3T3 GFP-actin fibroblasts, rosettes of individual podosomes emerge from an actin core that grows in diameter and splits into a rosette when it exceeds a crucial size, with a central area deprived of actin. When the rosette is formed, it moves in the cell with a specific speed, which is dependent upon the substrate rigidity. We observe that when rings of podosomes evolve near the cell periphery, they push the membrane, but latterly do not seem to influence either the stabilisation of the cell membrane protrusion nor the direction of cell migration (Fig. 7, supplementary material Movie 1). These observations appear to contradict recent work showing that such structures are associated with a migratory and invasive behaviour of cells (Osiak et al., 2005; Berdeaux et al., 2004; Buccione et al., 2004). Moreover, it is remarkable to note the concomitant expression of adhesive podosome groups and of more dynamically stable focal adhesions located at the extremities of actin stress fibres (Fig. 2C,D). The coexistence of these two types of actin-rich adhesive complex with different dynamics suggested two different functions. The first concerns the well-documented firm-adhesion process of fibroblasts, involving the setting of tension in actin fibres by the actomyosin motor, to acquire a spread, tensed cell structure. The second concerns a lesser-known way to explore the extracellular environment rapidly by the motion of podosome groups at the substrate-attached side. It seems logical that different cellular functions should involve different types of adhesion: focal adhesions with actin stress fibres to shape and tense the cell (Chen et al., 2003), and the swift group of podosomes with short actin filaments to explore, degrade and remodel the environment (Osiak et al., 2005; Linder and Aepfelbacher, 2003; Mizutani et al., 2002). Adhesive site dynamics appear to be tightly linked to matrix assembly and affected by the mechanical properties of the underlying substrate (Pelham and Wang, 1997; Zamir et al., 2000; Balaban et al., 2001). In fact, applying external physical tension near focal adhesions causes enlargement of these adhesive structures, thus exhibiting a dynamic relationship between applied force amplitudes on adhesion and the size and function of adhesions (Geiger et al., 2001; Riveline et al., 2001; Balaban et al., 2001). We showed here that individual podosome dynamics as well as the dynamics of podosome groups (i.e. the rosette) are also affected by the mechanical properties of the underlying matrix. It is therefore an attractive idea that podosome groups represent fast-moving mechanosensors, whereas focal adhesions behave as stable mechanotransmitters. Also, these highly dynamic podosome structures necessarily develop through an integrin-based sensing mechanism at the most intimate location where basal cell membrane and the ECM components interact (Fig. 2D), these interactions are mediated by the contractile proteins associated with the short actin filaments linked to the podosomes (Tanaka et al., 1993; Burgstaller and Gimona, 2004).

Using a cellular model expressing fluorescent molecules enables analysis of the dynamic organisation, fate and function of particular organelles or structure in living cells. Information provided by dynamic markers such as GFP-actin has promoted the development of dynamic methods to analyse image sequences. Previous methods were based on image-segmentation techniques, i.e. on the extraction of the points defining the object boundary at each time (Alt et al., 1995; Killich et al., 1994). Segmentation is particularly well suited to track local dynamic events. However, it cannot provide global information on the overall dynamics, such as the simultaneous movement of the many podosomes forming the rosette. We thus adopted a global approach using a parametric motion model, which turned out to be well adapted to quantify the distribution of apparent velocities of actin patterns induced by all individual podosome movement. This approach provides a rapid and efficient method to characterise the dynamic feature of the rosettes (expansion, contraction, oscillation). In addition, time-series data extracted from image sequences by this method can be directly analysed in order to detect the possible existence of periodic behaviour. The method is based on a light-conservation hypothesis, which is not completely the case because limited photo-bleaching occurs during the acquisition of time-lapse sequences. Nevertheless, we assumed that the bleach is negligible between two successive images and thus does not introduce a significant bias in the optical flow computation. This study provides an original analysis of ring-shaped rosette dynamics. Image analysis by an affine motion model of rosette movement allowed us to determine several parameters that have not been described until now and which characterise the dynamics of a specific group of podosomes.

Interestingly, the patterning of rosettes in cells appears not to be random. Actually, the spatial characteristics of the rosettes revealed that these structures are circular and present a continuous actin band of 4 μm width with a shape factor ranging from 1 to 2. FRAP experiments revealed that several rosettes exhibit constant flux with similar recovery times around 15 seconds, showing that very fast diffusion of actin occurs in the close vicinity of the rosette. Also, a rosette of podosomes exhibits oscillations induced by the disassembling and assembling of podosomes with constant periods (Fig. 9). These podosome rosette oscillations can exhibit different profiles: oscillations can be sustained for a long period of time, from 10 minutes to 1 hour, have a damping amplitude and are asymmetrical, i.e. with slow expansion phases and rapid shrinking phases (Fig. 9). Nevertheless, two harmonic periods have been identified, irrespective of substrate flexibility: one ~2 minutes, the other being ~4 minutes. This suggests that the rosette dynamics occur on a typical timescale of 2 minutes with a period doubling process, which in some cases slows down the dynamics. All together, these results indicate the existence of both characteristic time and space scales, which are known

signatures of self-organised systems (Nicolis and Prigogine, 1977; Strogatz, 1994). In this context, let us recall that several studies report that intracellular actin can exhibit highly dynamical patterns such as waves (Vicker, 2002), contractile rings (Guyader and Hyver, 1997) and that actin patterns express oscillatory properties actin clusters (Stephanou et al., 2004). However, the precise mechanisms underlying the self-organised dynamics of group of podosomes are still unclear. We hypothesise that a biochemical oscillator, based on the polymerisation-depolymerisation of actin polymers, leads to the formation of global-specific patterns of podosomes, such as the rosette. Considering that Arp2/3 is a podosome-related protein, and is known to have autocatalytic properties (Welch, 1999; Welch and Mullins, 2002), i.e. known to make actin polymerisation a far-from-equilibrium system, Arp2/3 is the main supposed actor for autocatalytic rosette propagation. Indeed, recent works report that Arp2/3-dependent branching polymerisation is necessary for actin wave propagation (Bretschneider et al., 2004) and Arp2/3 is also necessary for actin ring formation in osteoclasts (Hurst et al., 2004).

The second important finding is that the self-organised process we observed is bound by rules regarding the mechanical properties of the underlying substrate. Indeed, we have shown that the podosome lifespan decreases with substrate flexibility from 2 minutes 40±73 seconds for rigid substrates to 1 minute 24±38 seconds for a very flexible substrate, whereas the minimum distance *d* between podosomes increases from 1.53±0.36 μm for rigid substrates to 2.57±0.66 μm for very flexible substrates. Thus, local regulations linked to the substrate flexibility influence the properties of individual podosomes. A previous study has proposed that the global behaviour of podosome clusters is regulated by local mechanisms only, where a podosome could favour podosome formation at a short range while inducing a lasting inhibition at its exact location (Destaing et al., 2003). Thus a podosome could create an inhibition area directly around itself, but induces the formation of new podosomes beyond the inhibition zone (zi), these activation and inhibition mechanisms could be regulated by the different signalling pathways activated by the degree of maturity of the adhesive complex at the cell-substrate interface (Fig. 11). The adhesive complex maturity and their activation depend on the degree of substrate flexibility or external physical tension sensed, such as that shown for focal adhesions (Riveline et al., 2001; Paszek et al., 2005). Regarding the influence of microtubules in the inhibition zone that we discuss, it is known that microtubules stabilise podosome patterns (Babb et al., 1997; Linder et al., 2000). Nocodazole treatment has no effect on rosette formation and their persistence in our 3T3 cellular model. This result suggested that there is no influence of microtubules on the enlarged distance between podosomes seen on flexible substrates. This is not surprising, it has been already shown on mouse macrophages that de novo assembly of podosomes is not dependent on microtubules but the fusion and fission rates of larger precursor structures are based on microtubule dynamics (Evans et al., 2003). Destaing et al. have also demonstrated that a functional microtubule network was needed to stabilise the podosome belts at the cell periphery in osteoclasts (Destaing et al., 2003). Nevertheless, they showed, at early stages of osteoclast differentiation, that microtubule depolymerisation by nocodazole treatment has no visible effect on podosome clusters and rings.

Despite the lack of effect of the microtubule cytoskeleton on rosette formation, we observed the importance of the acto-myosin interaction for persistence and the de novo formation of podosomes group (Fig. 10). We propose that podosome behaviour is influenced by substrate stiffness by modulating the force balance generated by the contractility of acto-myosin complex and the counterpart resistance of the extracellular substrate.

In conclusion, the spatial organisation of the podosomes could be explained by a non-linear activation-inhibition process linked to the autocatalytic polymerisation of F-actin. In this scenario, dense actin clusters would be the precursor for podosome array formation. Then de novo actin formation and branching process mediated by ARP2/3 allow autocatalytic

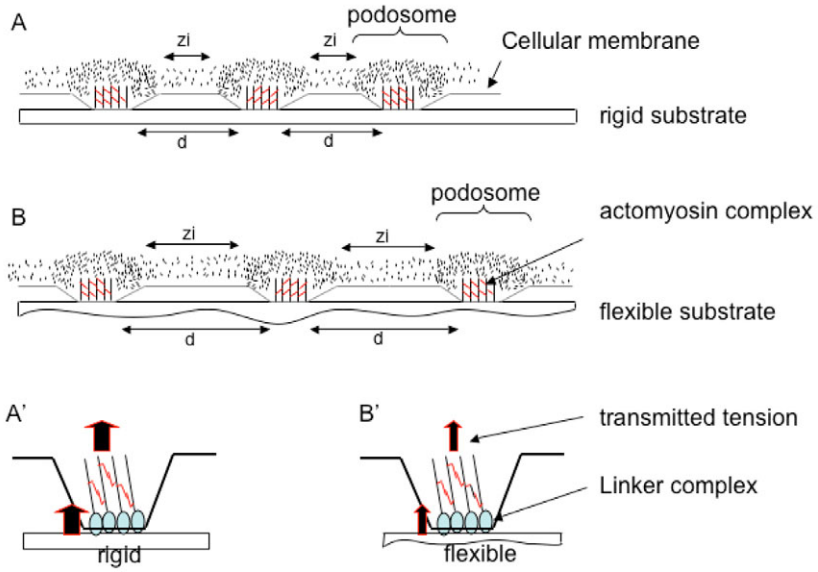

Fig. 11. Schematic representation of patterns of podosome groups adherent on rigid (A) or flexible (B) substrates. The zone of inhibition (zi) preventing the formation of new podosomes in a close vicinity of an existing podosome increases with the substrate flexibility. The reduction of contractile forces induced by the attachment to flexible substrate (B') compared with rigid substrate (A') should cause a cell-substrate immature adhesive interface at the podosome level and then reduce its lifespan and regulate minimum distance (d) between podosomes.

rosette formation and propagation. A second level of regulation is linked to the mechanical effects. Indeed the spatiotemporal patterning of podosomes in rosettes is dependent on the contractility mediated by the acto-myosin cytoskeleton; this patterning acting as a feedback on rosette propagation. In the context of far-from-equilibrium systems (Nicolis and Prigogine, 1977), it is understandable that an original podosome cluster could grow and expand in the form of a forward propagating wave of actin that triggers podosome formation. However, this does neither explain the further backward propagation of the podosome ring, nor the existence of oscillating forward/backward propagation revealed by the observed expending/contracting phases of the rosettes. Theoretical models based on assembly and disassembly of actin polymers then become essential for understanding the overall regulation of rosette formation as a multi-scale self-organisation process.

Materials and Methods

Cell culture and drug treatments

Mouse NIH 3T3 fibroblasts were obtained from a stable GFP-transfected actin clone cell. The cell culture medium was DMEM (Sigma Aldrich) with 4500 mg/l L-glucose, supplemented with 10% foetal calf serum (Invitrogen), 1% L-glutamine, 0.25% penicillin/streptomycin solution. The stability of the GFP-actin expression was maintained by 1 mg/ml gentamycin 418 (Sigma Aldrich). Nocodazol (Sigma Aldrich), 2,3-Butanedione monoxime (BDM; Sigma Aldrich) and cytochalasin D (Sigma Aldrich) were diluted into serum-containing media to obtain final concentrations at 10 μM, 20 mM, 1 μM respectively. (–)Blebbistatin (Calbiochem) was used in the same way with increasing concentrations from 50 to 100 μM. Control experiments were carried out under the same conditions using the DMSO in place of the drugs.

Polyacrylamide gel preparation

Polyacrylamide gels were prepared as previously described (Wang and Pelham, 1998). Briefly, gels were prepared with a 30% acrylamide solution and a 1% bis-acrylamide solution. Two different rigidities were obtained, according to the ratio 10% acrylamide/0.08% bis-acrylamide for very flexible gel or a 10% acrylamide/0.2% bis-acrylamide for flexible gel. The gel surfaces were functionalised with rat collagen-I (2 mg/ml). Cells were then seeded with 3000 cells/cm^2 in culture medium over the gel in the Petri dish and observed 24 to 48 hours after seeding.

Confocal microscopy and FRAP

Cell preparations were observed with a LSM 410 confocal scanning laser microscope (Carl Zeiss, Jena, Germany), using a 63×, NA 1.4, Plan-apochromat oil-immersion objective (Carl Zeiss). GFP-actin or Rhodamine-phalloidin fluorescence labelling were imaged with confocal fluorescence microscopy (CFM). FRAP experiments were carried out at 488 nm with maximum power of the argon laser for 10 seconds of bleaching. Fluorescence was collected with a 510-560 nm filter and fluorescence recovery analysis was made with the Metavue software (Meta Imaging Series 6.1, Universal Imaging, Downingtown).

Confocal interference reflection microscopy

Adhesion sites between cells and glass (focal adhesions and podosomes) were imaged in confocal interference reflection microscopy (CIRM) (Usson et al., 1997). The interference reflection images were obtained using a LSM 410 confocal scanning laser microscope (Carl Zeiss, Jena, Germany) with the polarised 488 nm line of an air-cooled argon laser. A rotating polariser was placed behind the confocal pinhole in order to reject internal light reflections from optical parts of the microscope. One confocal section per cell was recorded with the focus set to the level of interface between cell membrane and glass coverslip. This interface was found by changing the focus until the maximum of reflected light was obtained. Eight images were averaged in order to improve the signal-to-noise ratio. The images were coded over a 256 grey scale level.

Video microscopy

Live cultured cells adherent on glass or on gels were imaged with an inverted Axiovert 135 microscope (Carl Zeiss, Jena, Germany) equipped with an incubating chamber. Cells are thus maintained during the whole acquisition time in physiological conditions at 37°C and 5% CO_2 in a wet atmosphere. Images were recorded with a CDD coolsnap camera (Roper Scientific). We used 63×, NA 1.4, Plan-apochromat and 40×, NA 1.0, Plan-apochromat oil-immersion objectives (Carl Zeiss). GFP-actin-transfected cells were observed with a HBO 50W lamp passing through a GFP-specific filter (excitation 488 nm and emission 510 nm) (Carl Zeiss). Image analysis was performed with Metavue software (Meta Imaging Series 6.1, Universal Imaging, Downingtown) and ImageJ (National Institutes of Health, USA).

Analysis of actin-structure dynamics based on an optical flow method

The spatiotemporal analysis of the actin structures was realised with an optical flow method. The method is based on the direct exploitation of temporal and spatial variations of the light intensity observed for a sequence of images in a region of interest (ROI). This region was defined in our case as a rectangular area that isolated the actin structure to be studied.

A parametric affine motion model (Germain et al., 1999) was used to describe the dynamics of the actin structures. Thus, the apparent motion of each pixel $p(x,y)$ of the ROI was assumed to obey the following parametric relation:

$$w(p) = \begin{pmatrix} a_0 \\ a_3 \end{pmatrix} + \begin{pmatrix} a_1 & a_2 \\ a_4 & a_5 \end{pmatrix} \begin{pmatrix} x \\ y \end{pmatrix}, \quad (1)$$

where the time-dependent parameters a_0 and a_3 account for the rigid translation, whereas the parameters a_1, a_2, a_4 and a_5 of the matrix characterise the deformation field (Germain et al., 1999). This matrix can be also decomposed as follows (Zoccolan et al., 2001):

$$\begin{pmatrix} a_1 & a_2 \\ a_4 & a_5 \end{pmatrix} = E \begin{pmatrix} 1 & 0 \\ 0 & 1 \end{pmatrix} + \omega \begin{pmatrix} 0 & 1 \\ -1 & 0 \end{pmatrix} + S_1 \begin{pmatrix} 1 & 0 \\ 0 & -1 \end{pmatrix} + S_2 \begin{pmatrix} 0 & 1 \\ 1 & 0 \end{pmatrix}, \quad (2)$$

where $E=(a_1+a_5)/2$, $\omega=(a_2-a_4)/2$, $S_1=(a_1-a_5)/2$, $S_2=(a_2+a_4)/2$, are the expansion/contraction rate, the rotation rate, the horizontal and the oblique shear rates respectively.

Temporal analysis of rosettes oscillations

In order to detect the existence of any potential periodic components in the rosettes deformation dynamics, the Fourier transforms of the expansion/contraction curves E(t) were calculated in the following formulae:

$$(E)_n = \sum_{n=0}^{N} E_k e^{2i\pi kn/N}, \quad (3)$$

where N is the number of samples of the curve, E_k the amplitude for the sample k, and $(E)_n$ the amplitude for the frequency $\upsilon_n=n/T=n/(N\Delta t)$, with Δt the duration of the sampling interval. The signal energy was then given by $|(E)_n|$.

We thank Bernhard Wehrle-Haller for providing the 3T3 GFP-actin cell line. This research was supported by an Interdisciplinary Research Program 'complexity' of the French Centre National de la recherche Scientifique (CNRS). O.C. was supported by a doctoral fellowship from the Ministère de l'Education Nationale, de la Recherche et de la Technologie (MENRT, France) and E.P. by a visiting position from the CNRS.

References

Alt, W., Brosteanu, O., Hinz, B. and Kaiser, H. W. (1995). Patterns of spontaneous motility in videomicrographs of human epidermal keratinocytes (HEK). *Biochem. Cell Biol.* **73**, 441-459.

Babb, S. G., Matsudaira, P., Sato, M., Correia, I. and Lim, S. S. (1997). Fimbrin in podosomes of monocyte-derived osteoclasts. *Cell Motil. Cytoskeleton* **37**, 308-325.

Balaban, N. Q., Schwarz, U. S., Riveline, D., Goichberg, P., Tzur, G., Sabanay, I., Mahalu, D., Safran, S., Bershadsky, A., Addadi, L. et al. (2001). Force and focal adhesion assembly: a close relationship studied using elastic micropatterned substrates. *Nat. Cell Biol.* **3**, 466-472.

Beningo, K. A. and Wang, Y. L. (2002). Fc-receptor-mediated phagocytosis is regulated by mechanical properties of the target. *J. Cell Sci.* **115**, 849-856.

Berdeaux, R. L., Diaz, B., Kim, L. and Martin, G. S. (2004). Active Rho is localized to podosomes induced by oncogenic Src and is required for their assembly and function. *J. Cell Biol.* **166**, 317-323.

Bretschneider, T., Diez, S., Anderson, K., Heuser, J., Clarke, M., Muller-Taubenberger, A., Kohler, J., Gerisch, G. (2004). Dynamic actin patterns and Arp2/3 assembly at the substrate-attached surface of motile cells. *Curr. Biol.* **14**, 1-10.

Buccione, R., Orth, J. D. and McNiven, M. A. (2004). Foot and mouth: podosomes, invadopodia and circular dorsal ruffles. *Nat. Rev. Mol. Cell Biol.* **5**, 647-657.

Burgstaller, G. and Gimona, M. (2004). Actin cytoskeleton remodelling via local inhibition of contractility at discrete microdomains. *J. Cell Sci.* **117**, 223-231.

Burgstaller, G. and Gimona, M. (2005). Podosome-mediated matrix resorption and cell motility in vascular smooth muscle cells. *Am. J. Physiol. Heart Circ. Physiol*. **288**, H3001-H3005.

Burridge, K. and Chrzanowska-Wodnicka, M. (1996). Focal adhesions, contractility, and signaling. *Annu. Rev. Cell Dev. Biol.* **12**, 463-518.

Calle, Y., Chou, H. C., Thrasher, A. J. and Jones, G. E. (2004). Wiskott-Aldrich syndrome protein and the cytoskeletal dynamics of dendritic cells. *J. Pathol.* **204**, 460-469.

Chellaiah, M., Kizer, N., Silva, M., Alvarez, U., Kwiatkowski, D. and Hruska, K. A. (2000). Gelsolin deficiency blocks podosome assembly and produces increased bone mass and strength. *J. Cell Biol.* **148**, 665-678.

Chen, C. S., Mrksich, M., Huang, S., Whitesides, G. M. and Ingber, D. E. (1997). Geometric control of cell life and death. *Science* **276**, 1425-1428.

Chen, C. S., Alonso, J. L., Ostuni, E., Whitesides, G. M. and Ingber, D. E. (2003). Cell shape provides global control of focal adhesion assembly. *Biochem. Biophys. Res. Commun.* **307**, 355-361.

Chen, W. T. (1989). Proteolytic activity of specialized surface protrusions formed at rosette contact sites of transformed cells. *J. Exp. Zool.* **251**, 167-185.

Cukierman, E., Pankov, R., Stevens, D. R. and Yamada, K. M. (2001). Taking cell-matrix adhesions to the third dimension. *Science* **294**, 1708-1712.

David-Pfeuty, T. and Singer, S. J. (1980). Altered distributions of the cytoskeletal proteins vinculin and alpha-actinin in cultured fibroblasts transformed by Rous sarcoma virus. *Proc. Natl. Acad. Sci. USA* **77**, 6687-6691.

Deroanne, C. F., Lapiere, C. M. and Nusgens, B. V. (2001). In vitro tubulogenesis of endothelial cells by relaxation of the coupling extracellular matrix-cytoskeleton. *Cardiovasc. Res.* **49**, 647-658.

Destaing, O., Saltel, F., Geminard, J. C., Jurdic, P. and Bard, F. (2003). Podosomes display actin turnover and dynamic self-organization in osteoclasts expressing actin-green fluorescent protein. *Mol. Biol. Cell* **14**, 407-416.

Evans, J. G., Correia, I., Krasavina, O., Watson, N., Matsudaira, P. (2003). Macrophage podosomes assemble at the leading lamella by growth and fragmentation. *J. Cell Biol.* **161**, 697-705.

Folkman, J. and Moscona, A. (1978). Role of cell shape in growth control. *Nature* **273**, 345-349.

Gavazzi, I., Nermut, M. V. and Marchisio, P. C. (1989). Ultrastructure and gold-immunolabelling of cell-substratum adhesions (podosomes) in RSV-transformed BHK cells. *J. Cell Sci.* **94**, 85-99.

Geiger, B., Bershadsky, A., Pankov, R. and Yamada, K. M. (2001). Transmembrane crosstalk between the extracellular matrix–cytoskeleton crosstalk. *Nat. Rev. Mol. Cell Biol.* **2**, 793-805.

Germain, F., Doisy, A., Ronot, X. and Tracqui, P. (1999). Characterization of cell deformation and migration using a parametric estimation of image motion. *IEEE Trans. Biomed. Eng.* **46**, 584-600.

Guyader, H. L. and Hyver, C. (1997). Periodic activity of the cortical cytoskeleton of the lymphoblast: modelling by a reaction-diffusion system. *C. R. Acad. Sci. III Sci. Vie* **320**, 59-65.

Hurst, I. R., Zuo, J., Jiang, J. and Holliday, L. S. (2004). Actin-related protein 2/3 complex is required for actin ring formation. *J. Bone Miner. Res.* **19**, 499-506.

Kanehisa, J., Yamanaka, T., Doi, S., Turksen, K., Heersche, J. N., Aubin, J. E. and Takeuchi, H. (1990). A band of F-actin containing podosomes is involved in bone resorption by osteoclasts. *Bone* **11**, 287-293.

Kaverina, I., Krylyshkina, O. and Small, J. V. (2002). Regulation of substrate adhesion dynamics during cell motility. *Int. J. Biochem. Cell Biol.* **34**, 746-761.

Kaverina, I., Stradal, T. E. and Gimona, M. (2003). Podosome formation in cultured A7r5 vascular smooth muscle cells requires Arp2/3-dependent de-novo actin polymerization at discrete microdomains. *J. Cell Sci.* **116**, 4915-4924.

Killich, T., Plath, P. J., Hass, E. C., Xiang, W., Bultmann, H., Rensing, L. and Vicker, M. G. (1994). Cell movement and shape are non-random and determined by intracellular, oscillatory rotating waves in *Dictyostelium* amoebae. *Biosystems* **33**, 75-87.

Lauffenburger, D. A. and Horwitz, A. F. (1996). Cell migration: a physically integrated molecular process. *Cell* **84**, 359-369.

Linder, S. and Aepfelbacher, M. (2003). Podosomes: adhesion hot-spots of invasive cells. *Trends Cell Biol.* **13**, 376-385.

Linder, S. and Kopp, P. (2005). Podosomes at a glance. *J. Cell Sci.* **118**, 2079-2082.

Linder, S., Hufner, K., Wintergerst, U. and Aepfelbacher, M. (2000). Microtubule-dependent formation of podosomal adhesion structures in primary human macrophages. *J. Cell Sci.* **113**, 4165-4176.

Lo, C. M., Wang, H. B., Dembo, M. and Wang, Y. L. (2000). Cell movement is guided by the rigidity of the substrate. *Biophys. J.* **79**, 144-152.

Mizutani, K., Miki, H., He, H., Maruta, H. and Takenawa, T. (2002). Essential role of neural Wiskott-Aldrich syndrome protein in podosome formation and degradation of extracellular matrix in src-transformed fibroblasts. *Cancer Res.* **62**, 669-674.

Moreau, V., Tatin, F., Varon, C. and Genot, E. (2003). Actin can reorganize into podosomes in aortic endothelial cells, a process controlled by Cdc42 and RhoA. *Mol. Cell. Biol.* **23**, 6809-6822.

Mudera, V. C., Pleass, R., Eastwood, M., Tarnuzzer, R., Schultz, G., Khaw, P., McGrouther, D. A. and Brown, R. A. (2000). Molecular responses of human dermal fibroblasts to dual cues: contact guidance and mechanical load. *Cell Motil. Cytoskeleton* **45**, 1-9.

Mullins, R. D., Heuser, J. A. and Pollard, T. D. (1998). The interaction of Arp2/3 complex with actin: nucleation, high affinity pointed end capping, and formation of branching networks of filaments. *Proc. Natl. Acad. Sci. USA* **95**, 6181-6186.

Nicolis, G. and Prigogine, I. (1977). *Self-organization in Nonequilibrium Systems: From Dissipative Structures to Order through Fluctuations*. New York: Wiley.

Nobes, C. D. and Hall, A. (1995). Rho, rac, and cdc42 GTPases regulate the assembly of multimolecular focal complexes associated with actin stress fibers, lamellipodia, and filopodia. *Cell* **81**, 53-62.

Osiak, A. E., Zenner, G. and Linder, S. (2005). Subconfluent endothelial cells form podosomes downstream of cytokine and RhoGTPase signaling. *Exp. Cell Res.* **307**, 342-353.

Ostap, E. M. (2002). 2,3-Butanedione monoxime (BDM) as a myosin inhibitor. *J. Muscle Res. Cell Motil.* **23**, 305-308.

Paszek, M. J., Zahir, N., Johnson, K. R., Lakins, J. N., Rozenberg, G. I., Gefen, A., Reinhart-King, C. A., Margulies, S. S., Dembo, M., Boettiger, D. et al. (2005). Tensional homeostasis and the malignant phenotype. *Cancer Cell*. **8**, 241-254.

Pelham, R. J., Jr and Wang, Y. (1997). Cell locomotion and focal adhesions are regulated by substrate flexibility. *Proc. Natl. Acad. Sci. USA* **94**, 13661-13665.

Pelham, R. J., Jr and Wang, Y. L. (1998). Cell locomotion and focal adhesions are regulated by the mechanical properties of the substrate. *Biol. Bull.* **194**, 348-349.

Petit, V. and Thiery, J. P. (2000). Focal adhesions: structure and dynamics. *Biol. Cell* **92**, 477-494.

Pfaff, M. and Jurdic, P. (2001). Podosomes in osteoclast-like cells: structural analysis and cooperative roles of paxillin, proline-rich tyrosine kinase 2 (Pyk2) and integrin alphaVbeta3. *J. Cell Sci.* **114**, 2775-2786.

Riveline, D., Zamir, E., Balaban, N. Q., Schwarz, U. S., Ishizaki, T., Narumiya, S., Kam, Z., Geiger, B. and Bershadsky, A. D. (2001). Focal contacts as mechanosensors: externally applied local mechanical force induces growth of focal contacts by an mDia1-dependent and ROCK-independent mechanism. *J. Cell Biol.* **153**, 1175-1186.

Rottner, K., Hall, A. and Small, J. V. (1999). Interplay between Rac and Rho in the control of substrate contact dynamics. *Curr. Biol.* **9**, 640-648.

Saltel, F., Destaing, O., Bard, F., Eichert, D. and Jurdic, P. (2004). Apatite-mediated actin dynamics in resorbing osteoclasts. *Mol. Biol. Cell* **15**, 5231-5241.

Schamber, F. H. (1978). *Analysis of Environmental Samples*. Ann Arbor: X-Ray Fluorescence Publishers.

Schoenwaelder, S. M. and Burridge, K. (1999). Bidirectional signaling between the cytoskeleton and integrins. *Curr. Opin. Cell Biol.* **11**, 274-286.

Shu, S., Liu, X. and Korn, E. D. (2005). Blebbistatin and blebbistatin-inactivated myosin II inhibit myosin II-independent processes in Dictyostelium. *Proc. Natl. Acad. Sci. USA* **102**, 1472-1477.

Spinardi, L., Rietdorf, J., Nitsch, L., Bono, M., Tacchetti, C., Way, M. and Marchisio, P. C. (2004). A dynamic podosome-like structure of epithelial cells. *Exp. Cell Res.* **295**, 360-374.

Stephanou, A., Chaplain, M. A. and Tracqui, P. (2004). A mathematical model for the dynamics of large membrane deformations of isolated fibroblasts. *Bull. Math. Biol.* **66**, 1119-1154.

Strogatz, S. H. (1994). *Nonlinear Dynamics and Chaos: With Applications to Physics, Biology, Chemistry, and Engineering.* Reading, MA: Addison-Wesley.

Tanaka, J., Watanabe, T., Nakamura, N. and Sobue, K. (1993). Morphological and biochemical analyses of contractile proteins (actin, myosin, caldesmon and tropomyosin) in normal and transformed cells. *J. Cell Sci.* **104**, 595-606.

Tarone, G., Cirillo, D., Giancotti, F. G., Comoglio, P. M. and Marchisio, P. C. (1985). Rous sarcoma virus-transformed fibroblasts adhere primarily at discrete protrusions of the ventral membrane called podosomes. *Exp. Cell Res.* **159**, 141-157.

Tranqui, L. and Tracqui, P. (2000). Mechanical signalling and angiogenesis. The integration of cell-extracellular matrix couplings. *C. R. Acad. Sci. III Sci. Vie* **323**, 31-47.

Urech, L., Bittermann, A. G., Hubbell, J. A. and Hall, H. (2005). Mechanical properties, proteolytic degradability and biological modifications affect angiogenic process extension into native and modified fibrin matrices in vitro. *Biomaterials* **26**, 1369-1379.

Usson, Y., Guignandon, A., Laroche, N., Lafage-Proust, M. H. and Vico, L. (1997). Quantitation of cell-matrix adhesion using confocal image analysis of focal contact associated proteins and interference reflection microscopy. *Cytometry* **28**, 298-304.

Vicker, M. G. (2002). Eukaryotic cell locomotion depends on the propagation of self-organized reaction-diffusion waves and oscillations of actin filament assembly. *Exp. Cell Res.* **275**, 54-66.

Wang, Y. L. and Pelham, R. J. (1998). Preparation of a flexible, porous polyacrylamide substrate for mechanical studies of cultured cells. *Methods Enzymol.* **298**, 489-496.

Welch, M. D. (1999). The world according to Arp: regulation of actin nucleation by the Arp2/3 complex. *Trends Cell. Biol.* **9**, 423-427.

Welch, M. D. and Mullins, R. D. (2002). Cellular control of actin nucleation. *Annu. Rev. Cell Dev. Biol.* **18**, 247-288.

Yeung, T., Georges, P. C., Flanagan, L. A., Marg, B., Ortiz, M., Funaki, M., Zahir, N., Ming, W., Weaver, V. and Janmey, P. A. (2005). Effects of substrate stiffness on cell morphology, cytoskeletal structure, and adhesion. *Cell Motil. Cytoskeleton* **60**, 24-34.

Zamir, E., Katz, B. Z., Aota, S., Yamada, K. M., Geiger, B. and Kam, Z. (1999). Molecular diversity of cell-matrix adhesions. *J. Cell Sci.* **112**, 1655-1669.

Zamir, E., Katz, M., Posen, Y., Erez, N., Yamada, K. M., Katz, B. Z., Lin, S., Lin, D. C., Bershadsky, A., Kam, Z. et al. (2000). Dynamics and segregation of cell-matrix adhesions in cultured fibroblasts. *Nat. Cell Biol.* **2**, 191-196.

Zoccolan, D., Giachetti, A. and Torre, V. (2001). The use of optical flow to characterize muscle contraction. *J. Neurosci. Methods* **110**, 65-80.

Journal of Cell Science